Borated graphite cathodes for low-temperature aluminum electrolysis

Rudenko A.V. a* , Kataev A.A. a , Neupokoeva M.M. ab, Tkacheva O.Yu. ab

a: Institute of High Temperature Electrochemistry, Ural Brunch of Russian Academy of Sciences, Ekaterinburg 620137, Russia
b: Ural Federal University named after the first President of Russia B.N. Yeltsin, Ekaterinburg 620002, Russia
* Corresponding author: a.rudenko@ihte.uran.ru

This paper belongs to a Regular Issue.

Abstract

Electrochemical boriding of the graphite plates in the potassium cryolite based electrolytes was studied. The boriding were carried out in a cell with vertical electrodes. The procedure included 2 stages: 1) electrolysis in the $KF–AlF_3–KBF_4$ melt (CR=1.3) at low current density (0.01–0.02 A/cm^2), required for the boron reduction, at 700 and 750 °C; 2) electrolysis in the $KF–AlF_3–Al_2O_3$ melt at higher current density (0.2 A/cm^2), required for the aluminum reduction. The optimal conditions of electrodeposition for obtaining the borated wettable cathodes were determined. According to the SEM data, a continuous AlB_2 layer with a thickness of 7–10 μm was formed on the graphite surface. The borated graphite was tested as a wetted cathode during the low-temperature aluminum electrolysis. Prolonged electrolysis in a vertical cell with the graphite anode and the borated graphite cathode was carried out in the $KF–NaF(10 wt.\%)–AlF_3–Al_2O_3$ electrolyte (CR=1.5) at 830 °C. After 100 h of electrolysis, the thickness of the AlB_2 layer on the graphite surface was 5 μm, while the cathode surface was completely wetted with aluminum. Thus, we demonstrated the feasibility of using the borated graphite cathode as a wettable dripping cathode in the low-temperature aluminum electrolysis in the vertical cell.

1. Introduction

Nowadays, almost all primary aluminum is obtained by the Heroult-Hall process, which has not undergone any fundamental changes during more than 100 years [1]. The technology consists in the electrolytic decomposition of alumina dissolved in sodium cryolite (Na_3AlF_6 with additions of AlF_3, CaF_2, etc.) at 940–970 °C. It is worth noting that aluminum production is an extremely energy-consumption process: the cost of electricity is more than 30%. The process is accompanied by the consumping of carbon anodes and the emission of a significant amount of harmful gases (CO, CO_2 and freons) that create a greenhouse effect [2, 3]. A radical modification of the Heroult-Hall process is possible by replacing consumable carbon anodes with non-consumable inert anodes [4]. However, as of now, there is no information regarding the successful application of inert anodes in conventional technology. The main reason for this is the aggressiveness of the cryolite-alumina melt at high temperatures. To prevent fast corrosive destruction of structural materials, it is necessary to reduce the operating temperature of the process. In this regard, it becomes necessary to create and develop a new technology for low-temperature aluminum electrolysis. Its main advantages would be energy saving, a significant reduction in greenhouse gas emissions and an increase of the cell life. In addition, the solubility of metallic aluminum in the molten electrolyte decreases with reducing temperature [5], which will lead to an increase in the current efficiency.

Attempts to develop a low-temperature process for producing aluminum were focused on modifying the conventional electrolyte based on sodium cryolite: lowering the temperature was achieved mainly by increasing the aluminum fluoride content. However, due to the low solubility of alumina in such melts, they have not found application in the industry.

Another way of solving the problem is using an electrolyte based on potassium cryolite. The physicochemical properties of such melts are well studied [6–8]. The $KF–AlF_3$ mixtures with cryolite (molar) ratio (CR) $(CR=X(KF)/X(AlF_3))$ from 1.3 to 1.5 have a liquidus temperature below 800 °C and the solubility of alumina that is higher than in the sodium system. The low-temperature electrolysis in electrolytes, the main component of which is potassium cryolite, was demonstrated by several researchers [9–13].

In the low-temperature aluminum electrolysis inert anodes are used instead of graphite anodes. The inert anodes must meet certain requirements: low solubility in cryolite melts, high electrical conductivity, easy machining, and low cost. The metal anodes fulfill all requirements and are, therefore, the subject of special attention. As a rule, the composition of the material for inert metal anodes is based on the Cu–Al or Cu–Fe–Ni alloys [14–17].

The low-temperature electrolysis with inert anodes requires a new operation system of the electrolytic process and a new cell design, specifically, the use of cells with vertically arranged electrodes. Such design, according to preliminary calculations, will reduce energy consumption by 25%, increase the current efficiency, while maintaining a high density current, and reduce the cell size [17, 18].

Beck [9, 18] carried out the long-term (300 h) electrolysis in the $KF–AlF_3$ molten eutectic and the $KF–AlF_3$ and $NaF–AlF_3$; the temperature varied from 700 to 850 °C. Although Al_2O_3 was added in an amount of 10 wt.%, the actual concentration of dissolved alumina was about 4 wt.% (as follows from the figures of report [18]). The 10, 200 and 300 A cells were equipped with the Cu–Ni–Fe anodes and the TiB_2 cathodes. It was reported that current efficiency reached 95%, and the purity of aluminum was 99.5% in 200-ampere cell.

The electrolysis in the $(45wt\%)KF–AlF_3–(5wt\%)Al_2O_3$ melt with CR=1.3 was successfully performed at 700 and 750 °C in the 10, 20 and 100 and 1000 A vertical cells [10, 11]. Aluminum bronze was served as the anode, and the $TiB_2–C$ composite was used as the cathode. The same electrolyte composition was used in electrolysis tests in a cell with the Cu–Ni–Fe inert anodes at 700 °C [15].

However, in addition to the issues concerning corrosion-resistant material for inert anodes, the composition of low-melting electrolyte, etc., the necessity in the material of vertical cathodes with good wettability and corrosion resistance in fluoride melts arises. In addition, several researchers have noted the problem of cathode passivation during low-temperature electrolysis [19–21]. The cathode material should be thermally and chemically stable under electrolysis conditions, but, perhaps, the most important requirement is a good wettability of the cathode surface by the liquid aluminum [22].

It is known that the titanium diboride is the best material for a wetted cathode. Cathodes made of TiB_2 or $TiB_2–C$ composite are well suited for a vertical cell design. Brown [23] investigated materials $TiB_2–B_4C$, $TiB_2–BN$, $TiB_2–TiC$ under electrolysis conditions. The cathodes were prepared using different techniques. The performance of the cathode material was evaluated by the values of current efficiency compared to commercial HP TiB_2. It was found that no one material has performed better than TiB_2. However, it should be noted that the TiB_2 is very difficult to machine, and its cost is also high. Therefore, the search for new materials for wettable cathodes for the low-temperature aluminum electrolysis remains an urgent task.

The electrolytic methods of applying a boride coating on cathodes for the electrolytic aluminum production, including the electrodeposition of boron and titanium in the form of titanium diboride on graphite and other materials, were described in [24, 25]. The electrodeposition was performed in fluoride and chloride-fluoride melts at 650–710 °C, using the K_2TiF_6 and KBF_4 salts as sources of titanium and boron. The resulting coatings were characterized by a good adhesion to the cathode and relatively high erosion and chemical resistance in molten salts.

The electrochemical boriding of steel in a borax-based molten electrolyte at 950 °C was considered in works [26, 27]. It was described that this process yielded a very dense, uniform, and hard boride layer.

The authors [28] studied the electrochemical behavior of boron in a melt $KBF_4–LiF–NaF–KF$ at 700 °C and found that boron interacts with the surface of the working electrode, which was glassy carbon, platinum, or silver.

Ray [29] discovered that small additions of TiO_2 and B_2O_3 to the cryolite-based melt $(Na_3AlF_6–Al_2O_3–CaF_2)$ at about 1000 °C increase the wettability of the graphite electrode by molten aluminum due to formation of Al–Ti or Al–B alloys on the graphite surface. Moreover, the Al–B alloy improves the wettability of graphite more efficiently.

The authors [30] compared the wettability of borated steel and hot pressed TiB_2 in terms of the wetting angle. A sample of borated steel was obtained in two stages: first, by boriding steel in a borax melt; then aluminizing was carried out by the thermal diffusion saturation. They found that the borated steel was wetted better by the liquid Al than the TiB_2. However, it was noticed that the properties of TiB_2 largely depend on the preparation technique.

Kataev [31] found that during electrolysis in the $KF–AlF_3–B_2O_3$ melt at 700 °C in cells with graphite electrodes a layer of the AlB_2 intermetallic compound was formed on the surface of graphite cathode, which significantly improved the wettability of C-cathode with liquid aluminum.

Thus, it can be concluded that borated graphite, probably, surpasses even titanium diboride in wettability with the liquid aluminum, and the boron coatings on graphite can be obtained by electrolysis of molten salts.

The objectives of this work were: (i) to determine the operating parameters for obtaining a boride coating on graphite cathode by electrolysis in the $KF–AlF_3–KBF_4$ melt; (ii) to test a wetted cathode in a cell with vertically arranged electrodes during the low-temperature aluminum electrolysis.

2. Experimental

2.1. Chemicals

The melts were prepared from the reagent-grade NaF, KF·HF, AlF$_3$(99%), KBF$_4$ (99%), Al$_2$O$_3$ supplied by Vekton Ltd (Russia).

The KF–AlF$_3$–KBF$_4$ melt was used as a medium for the electrochemical boriding. The KF–AlF$_3$ electrolyte with a cryolite ratio (CR=X(KF)/X(AlF$_3$)) of 1.3 was obtained by mixing the KF·HF and AlF$_3$ salts (in a glassy carbon container). The mixture was exposed to 750 °C over 4 h in order to remove the HF from the melt due to the thermal decomposition of the KF·HF. The electrolyte preparation process is described in detail elsewhere [8]. The amount of "O" in the prepared electrolyte was determined by the carbothermal reduction technique using an oxygen analyzer LECO TC836. It was found that the original electrolyte contained 0.6 wt.% "O", which corresponds to 1.25 wt.% Al$_2$O$_3$.

The molten mixture KF–NaF(10 wt.%)–AlF$_3$ with CR=1.5 (CR=(X_{KF} + X_{NaF})/X_{AlF_3}) was used for prolonged 100 h electrolysis in order to test efficiency of the borated graphite cathode.

The KF–AlF$_3$–KBF$_4$ electrolyte was chosen for boriding because it has a significantly lower liquidus temperature than the KF–NaF(10 wt.%) –AlF$_3$ molten mixture [7]. This provided a low operating temperature and, consequently, a lower degree of the thermal decomposition of KBF$_4$ with the release of gaseous BF$_3$. In addition, it is known [32, 33] that NaBF$_4$ is more susceptible to the thermal decomposition than KBF$_4$; that is, the presence of NaF in the electrolyte is undesirable.

On the other hand, the electrolyte KF–NaF(10 wt.%)–AlF$_3$ was recommended for the low-temperature electrolysis because it has a higher alumina solubility [7]. It should be noted that the operating temperature of electrolysis in this electrolyte is higher than 800 °C; however there is no so-called "sodium problem" associated with the accumulation of NaF, which enters the electrolyte as an alumina impurity, and is accompanied by a significant increase in the operating temperature [7].

2.2. Electrochemical cell

Boriding the graphite cathode as well as testing a wettable cathode under electrolysis conditions was carried out in the vertical cell. The procedures for these processes have some differences, as will be indicated below. However, the design of the cell remained the same. A schematic diagram of the electrochemical cell is presented in Figure 1. Dense graphite served as the anode. Graphite or borated graphite was used as the cathode. The anode-cathode distance was 20 mm. The dimensions of the electrodes were 20x70x8 mm. The electrodes were not completely immersed in the melt, but to a depth of 75 mm. The current density was calculated on the surface area facing the anode. For reliable electrical contact the current leads (steel) were

screwed into the threaded electrodes. The current leads were protected from interaction with the atmosphere by alumina cases. The salt mixture (about 400 g) was placed into the alumina crucible (V=600 ml). The alumina powder was filled between the crucible and the container. The experiments were carried out in an open cell in ambient air.
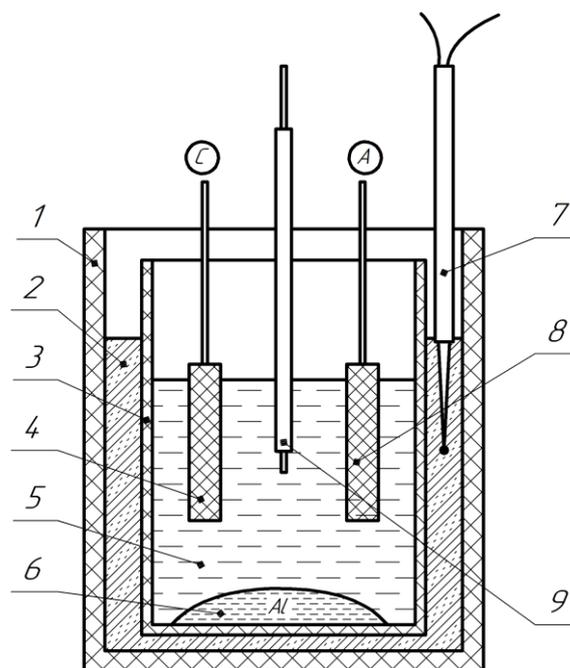

Figure 1 Schematic diagram of an electrochemical cell: 1 – protective alumina container; 2 – alumina backfill; 3 – alumina crucible; 4 – cathode; 5 – electrolyte; 6 – liquid aluminum; 7 – Pt/Pt–Rh thermocouple; 8 – carbon anode; 9 – two tungsten quasi-reference electrodes in alumina case.

The temperature of the cell was measured by Pt–Pt/Rh thermocouple using an APPA 109N multimeter. The potential between the anode, the cathode and W quasi-reference electrodes was measured and recorded using an APPA 109N multimeter. The electrolysis was performed with the help of an Autolab PGSTAT 302 with a BSTR20A booster.

2.3. Boriding

A boride coating on a graphite cathode was obtained by electrolysis in the KF–AlF$_3$–KBF$_4$ melt.

It was evaluated in [33] that in the potassium cryolite melt with the addition of 15 mol.% KBF$_4$ the loss of boron due to the thermal decomposition does not exceed 3% in the temperature range of 400–800 °C. However, taking into account the possible low boron current efficiency, the addition of KBF$_4$ was made in excess. The KBF$_4$ component was added to the KF–AlF$_3$ electrolyte in amount of 0.5 wt.%, that ten times exceeded the calculated value for the formation of AlB$_2$ layer (10 μm) at the boron current efficiency of 100%. It should be noted that the boron concentration in the electrolyte during boriding was not analyzed.

The current density was 0.01 and 0.02 A/cm², and temperature was varied from 700 to 750 °C. The choice of such a low current density was based on the results of the work [31]. The authors determined the operating parame-

ters for the production of Al–B alloy by electrolytic reduction of B_2O_3 in the KF–AlF$_3$–Al$_2$O$_3$ melt: the initial current density was 0.02 A/cm^2 at 700 ºC.

In order to identify the boride layer by scanning electron microscope (SEM) the electrolysis process was continued at a higher current density. The alumina in amount of 3 wt.% was added to the electrolyte. An aluminum layer on top of the boron facilitated the determination of the presence and thickness of the boron on graphite against the background of aluminum. Cross-section of the borated cathode was analyzed using the SEM with nitrogen-free energy dispersive detector X-act ADD+JSM- 5900LV supplied with a wave dispersive micro analyzer, sluice chamber and a device for suppression of electromagnetic interference INCA Energy 250 and INCA Wave 500.

2.4. Electrolysis test

The borated cathodes were tested under the conditions of the low-temperature aluminum electrolysis in the KF–NaF(10 wt.%)–AlF$_3$–Al$_2$O$_3$ melt with CR = 1.5. The anode was graphite. As it was consumed, the anode was replaced with a new one. Electrolysis parameters were as follows: current density i = 0.2 A/cm^2, temperature 830 ºC. The current density was chosen based on the results of work [34], in which it was recommended not to increase the cathode current density above 0.35–0.5 A/cm^2 in order to avoid the formation of solid deposits on the cathode. As indicated by the authors, at the current density of 0.2 A/cm^2, the current efficiency in the vertical cell was about 67%. Thus, in the present work the amount of added Al$_2$O$_3$ during electrolysis was calculated assuming 60% current efficiency in order to maintain the Al$_2$O$_3$ concentration in the electrolyte at 2–3 wt.%. During electrolysis, liquid aluminum drips from the cathode and forms a pool at the bottom of the cell (Figure 1). The potential differences between the cathode and the W quasi-reference electrode and between the anode and the W quasi-reference electrode were measured during electrolysis. They were used only to identify possible malfunctions of either the anode or the cathode.

3. Results and Discussion

3.1. Boriding the graphite cathode

A wettable coating on the graphite cathode was obtained by electrolysis in the KF–AlF$_3$–KBF$_4$ melt. The current density and operating temperature were varied.

According to the data [35], the boron may be electrochemically deposited from the cryolite-based electrolyte (Na$_3$AlF$_6$ + 1 wt.% Al$_2$O$_3$ + 0.2 wt.% B$_2$O$_3$, 1050 ºC) at lower voltage that that required for the aluminum reduction. The difference between the reduction potentials is reported to be about 0.6 V. The authors [36] recommend performing the boron electrodeposition in the KF–AlF$_3$–Al$_2$O$_3$–B$_2$O$_3$ (CR=1.3) melt at potentials 0.6 V more positive than the aluminum reduction potential (at 750 ºC).

Since there is a small amount of oxygen ions in the original electrolyte (as stated above), the oxidation process of the oxygen-containing ions occurs at the graphite anode with the formation of CO_2.

Considering that boron is in the ionic melt in the form of a complex anion BF^{4-} [37], the cathode process can be described by the following equation:

$$BF^{4-} + 3e = B + 4F^{--} \qquad (1)$$

During the deposition of aluminum, the interaction of Al and B with the formation of intermetallic compounds (AlB$_2$, AlB$_{12}$) can occur [38]. According to the Al–B phase diagram, at a temperature of about 750 ºC, it is possible to obtain Al–B alloys containing at least 0.09% boron.

Thus, the process of obtaining a wettable cathode took place in 2 stages.

Stage 1: The objective of the first stage was to obtain a boron coating on the graphite cathode. The electrolysis in the KF–AlF$_3$–KBF$_4$ melt with CR=1.3 was carried out in a galvanostatic mode at low current densities required for boron reduction at 700 and 750 ºC. The electrolysis time was varied, while the charge in all experiments remained constant and equal to 0.6 C.

Stage 2: The goal of the second stage was to deposit the aluminum at the cathode in order to obtain an aluminum-boron coating. The electrolysis in the KF–AlF$_3$–Al$_2$O$_3$ CR=1.3 melt was carried out in a galvanostatic mode at higher current densities required for the production of aluminum. The duration and current density in all experiments were the same.

The parameters of two-staged electrolysis are summarized in Table 1. Four series of experiments were carried out. In each series, the electrolysis proceeded stably, the voltage was constant both at the first and at the second stages of electrolysis (Figure 2).

The images of the coating obtained on graphite in exp.1 with i = 0.02 A/cm^2 at 700 ºC and the boron distribution map in the aluminum matrix are given in Figure 3. The boron is represented in red. The thickness of the Al layer was 800 µm. A continuous boron layer, 7–10 µm thick, was formed on the graphite surface. The enlarged spectrum shown in Figure 3b indicates that in the dark areas (spectrum 1, 3, 7, 9) the B content was about 63 at.% and the Al content was about 33 at.%, which corresponds to AlB$_2$. The grain size of AlB$_2$ was 3–5 µm.

Table 1 Parameters of two-stage electrolysis for obtaining boride coating on graphite.

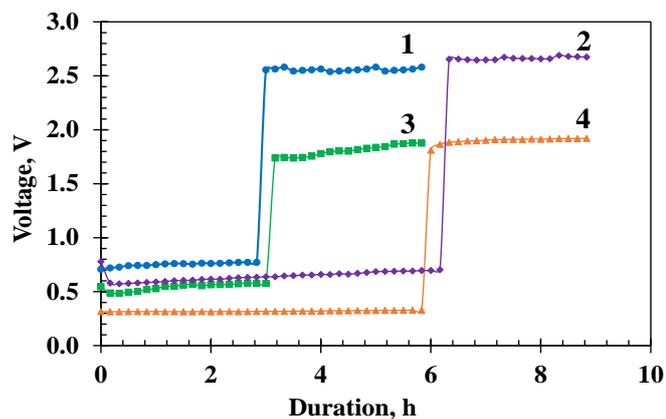| Parameters	Stage 1				Stage 2
	exp.1	exp.2	exp.3	exp.4	
Electrolyte	KF–AlF$_3$–KBF$_4$, CR=1.3				KF–AlF$_3$–Al$_2$O$_3$, CR=1.3
Addition	KBF$_4$ 0.5 wt.%				Al$_2$O$_3$ 3 wt.%
Temperature, ºC	700	700	750	750	700–750
Current density, A/cm^2	0.02	0.01	0.02	0.01	0.2
Duration, h	3	6	3	6	3

Figure 2 Voltage in two-stage electrolysis: 1 – exp.1; 2 – exp.2; 3 – exp.3; 4 – exp. 4 (Table 1).
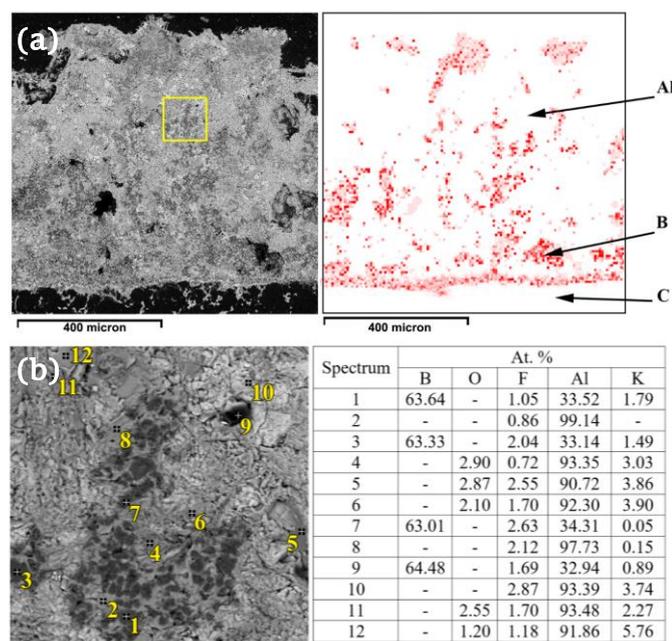

Figure 3 Image of the aluminum layer and the boron distribution map obtained in exp. 1 (a); enlarged area of the image (a) (yellow square).

In exp.2 under the same conditions, but with a decrease in current density and an increase in duration by a factor of 2, the boron distribution changed (Figure 4), while the thickness of the Al layer remained the same (800 μm). The boron was distributed uniformly over the thickness of the aluminum layer; however, no continuous uniform boron layer covering the graphite surface was found.

With an increase in the electrolysis temperature to 750 °C and at i = 0.02 and 0.01 A/cm^2 (exps. 3 and 4), the boron is almost absent from the aluminum layer (Figure 5). The thickness of the aluminum layer on graphite is 600 and 370 μm, respectively.

For testing the coating cathodes under conditions of prolonged electrolysis, the cathode obtained in exp. 1 was chosen. It had the thickest aluminum layer and uniform boride coating on the graphite surface.
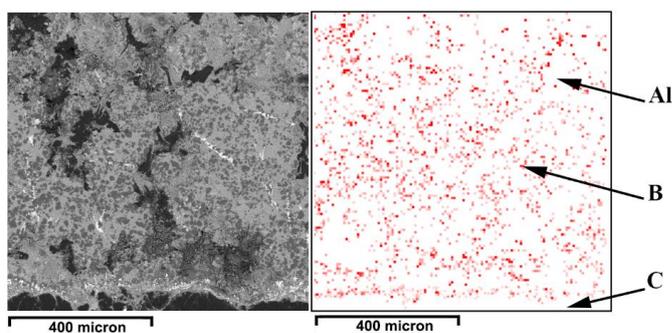

Figure 4 Image of the aluminum layer and the boron distribution map obtained in exp. 2.
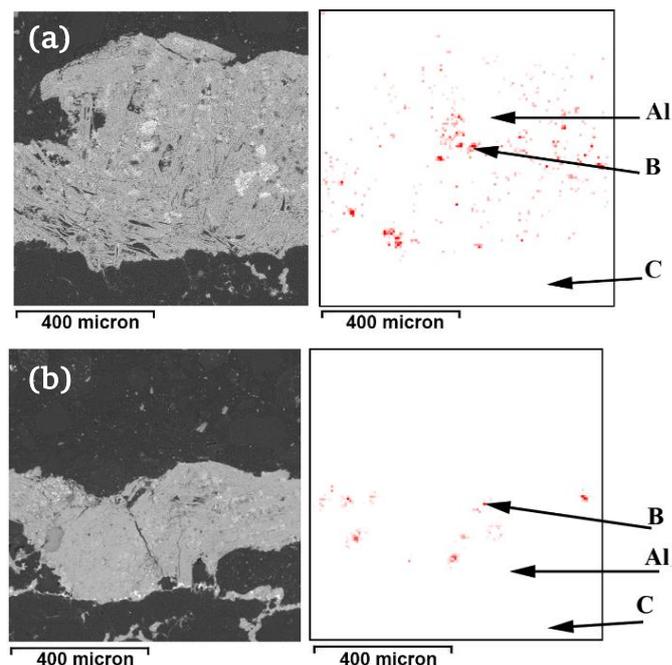

Figure 5 Images of the aluminum layer and the boron distribution map obtained at 750 °C at the current density of 0.02 (a) and 0.01 (b) A/cm^2.

Thus, a twofold decrease in the current density at the same temperature leads to a more uniform distribution of the intermetallic compound AlB$_2$ over the thickness of the aluminum coating. An increase in temperature by 50 °C under the given electrolysis conditions prevents the formation of boride coatings on the graphite surface.

It should be noted that for all the parameters of the two-stage electrolysis, the aluminum formed in the second stage wetted well and was evenly distributed over the surface of the graphite cathode. The only differences were that, depending on the electrolysis parameters applied, the thickness of the aluminum layer, the uniformity of the boron distribution in the aluminum layer and its amount changed. For comparison, uncoated graphite was used as the cathode in the vertical cell. The electrolysis was carried out for 50 h. The photos of the graphite cathode before and after electrolysis are shown in Figure 6. The cathode was covered with aluminum droplets, indicating that the graphite surface was not wetted by the Al metal.

Figure 6 Uncoated graphite cathode before and after aluminum electrolysis in vertical cell.

3.2. Test of wettable cathode during the aluminum electrolysis

The test of the borated graphite cathode were carried out in the KF–NaF(10 wt.%)–AlF$_3$–Al$_2$O$_3$ melt with CR=1.5 at 830 ℃ for 100 h (in total). The electrolysis with the same cathode was carried out in two steps: the duration of the first step was 75 h and the second step lasted for 25 h.

The voltage and potentials of the cathode and the anode during electrolysis are given in Figure 7.

The electrolysis was sustained, the voltage at step 1 was ~2.1 V. The cathode potential was stable. The increase in the anode potential by 38th, 49th, and 62nd h of electrolysis is associated with the consumption and replacement of the graphite anodes. At the second step, the voltage systematically increased from 2.1 to 2.3 V. It appears from the symbatic nature of curves trend of the voltage and the anode potential that the increase in voltage is associated precisely with the operation of the inert anode. The increase in voltage after 21st h of electrolysis

is explained by the breakdown in the contact of the current lead with the anode.

After each step of electrolysis, the lower part of the cathode was cut off and a cross-section was prepared for a metallographic examination. An image of the cathode section after 75 h of electrolysis is shown in Figure 8a. The dark gray areas in the image are AlB$_2$, the lighter areas contain less boron. The boride coating layer AlB$_2$ is preserved, its thickness is 7 µm. The grains are distributed uniformly over the thickness of the Al layer.

An image of the cathode cross-section after 100 h of electrolysis is presented in Figure 8b. The thickness of the AlB$_2$ coating on the graphite surface after 100 h (Figure 8b) is about 5 µm. It can be assumed that boron dissolves in molten aluminum. Based on the SEM data, it was calculated that about 0.0028 g of boron was transferred from the cathode surface to the volume of molten aluminum during 25 h of electrolysis (Figure 8b).

An external examination of the cathode after the experiment did not reveal any damage. An image of the cross-section of the graphite cathode with the diboride coating after electrolysis is shown in Figure 9.

The cathode surface was completely wetted with aluminum. The thickness of the aluminum layer was 2 mm. Detachment of the aluminum from the cathode surface is not observed, which indicates good wetting of the graphite surface with aluminum.

The current efficiency was 62 %.

Thus, the prolonged 100-h electrolysis tests of the graphite cathode, previously coated with the aluminum diboride, in the vertical cell proved its efficiency.

Undoubtedly, tests of wetted cathodes should be continued under conditions of longer electrolysis duration. However, it should be noted that, if necessary, an additional boriding of the cathode can be carried out during low-temperature aluminum electrolysis without changing its parameters.
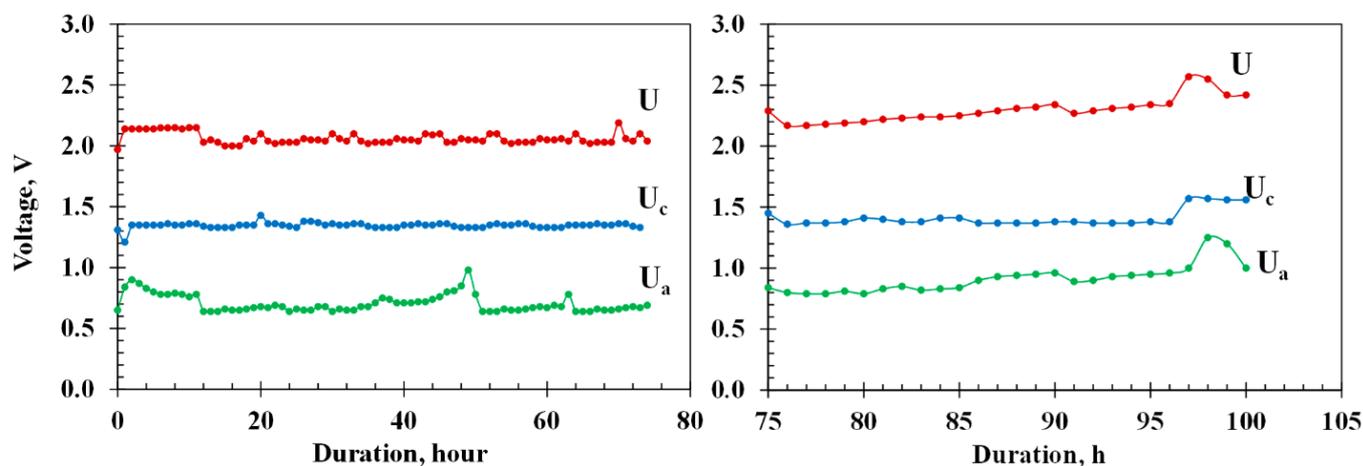

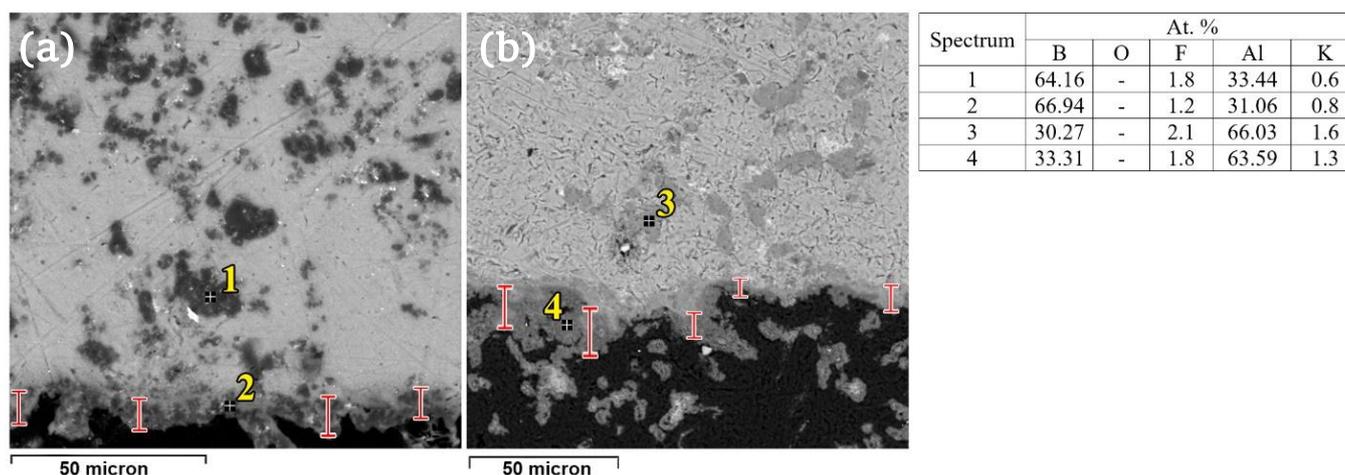**Figure 7** Voltage during electrolysis in the vertical cell with wetted borated graphite cathode.

Spectrum	At. %				
	B	O	F	Al	K
1	64.16	-	1.8	33.44	0.6
2	66.94	-	1.2	31.06	0.8
3	30.27	-	2.1	66.03	1.6
4	33.31	-	1.8	63.59	1.3

Figure 8 Images of the borated cathode after 75 h (a) and 100 h (b) of electrolysis.

a   b
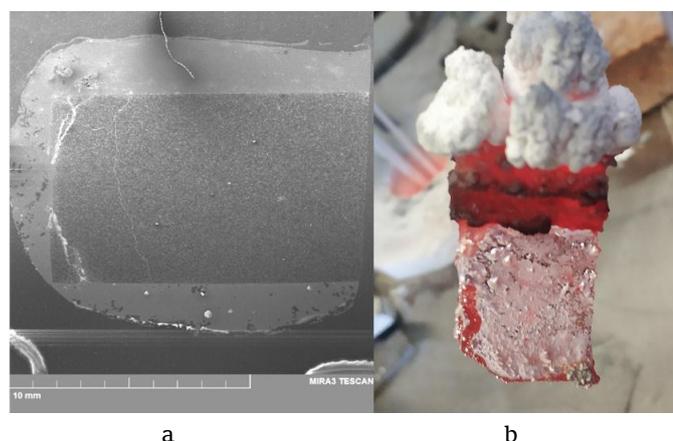
Figure 9 Image of cross-section (a) and general view of the hot wetted cathode after 100h electrolysis (b).

4. Conclusions

Boriding the graphite plates was accomplished by electrolysis in the KF–AlF$_3$–KBF$_4$ melt (CR=1.3) in two stages. At the first stage, the boron was reduced at the graphite cathode at the current density of 0.01 and 0.02 A/cm^2 and temperature 700 and 750 ºC, and at the second, the aluminum was deposited at the current density of 0.2 A/cm^2. The second stage was necessary in order to improve the identification of boron against the background of the aluminum by SEM. The operating parameters for the electrochemical deposition of continuous boride coatings on the graphite surface were found. Nevertheless, despite the different values of the parameters of two-stage electrolysis, in all cases, aluminum, being reduced in the second stage of the process, wetted the graphite surface well. The difference was found only in the thickness of the aluminum layer and the amount and distribution of boron in the aluminum layer.

The test of the borated graphite cathode under conditions of the low-temperature electrolysis in the KF–NaF(10 wt.%)–AlF$_3$–Al$_2$O$_3$ (CR=1.5) melt at 0.2 A/cm^2 and 830 ºC for 100 h confirmed the possibility of its use as a wetted dripping cathode in the electrolytic production of aluminum in low-melting cryolite.

Author contributions

Conceptualization: K.A.A., T.O.Yu.
Data curation: T.O.Yu.
Formal Analysis: R.A.V., K.A.A., T.O.Yu.
Funding acquisition: R.A.V., T.O.Yu.
Investigation: R.A.V., K.A.A., N.M.M.
Methodology: R.A.V., K.A.A.
Project administration: R.A.V.
Resources: R.A.V., K.A.A.
Software: R.A.V., K.A.A.
Supervision: T.O.Yu.
Validation: R.A.V., T.O.Yu.
Visualization: R.A.V.
Writing – original draft: R.A.V., T.O.Yu.
Writing – review & editing: R.A.V., T.O.Yu.

Conflict of interest

The authors declare no conflict of interest.

Additional information

Author ID's:
Rudenko A.V., Scopus ID 57197500558;
Kataev A.A., Scopus ID 12241606800;
Tkacheva O.Yu., Scopus ID 6602941818.

Websites:

Institute of High Temperature Electrochemistry, UB RAS, http://www.ihte.uran.ru/?page_id=3118;

Ural Federal University, https://urfu.ru/en.

References

1. Haupin WE. Principles of aluminum electrolysis. Essent Read Light Met. 2016;2(3):3–11. doi:10.1007/978-3-319-48156-2_1

2. Evans J, Kvande H. Sustainability, climate change, and greenhouse gas emissions reduction: Responsibility, key challenges, and opportunities for the aluminum industry. JOM. 2008;60(8):25–31. doi:10.1007/s11837-008-0103-2

3. Leber BP. Perfluorocarbon (PFC) generation at primary aluminum smelters. Essent Read Light Met. 2016;2:1015–1023. doi:10.1007/978-3-319-48156-2_150

4. Galasiu I, Galasiu R, Thonstad,J, Inert anodes for aluminium electrolysis. Aluminium-Verlag. 2007. 207 p.

5. Thonstad J. The solubility of aluminium in $NaF–AlF_3–Al_2O_3$ melts. Can J Chem. 1965;43:3429. doi:10.1139/v65-476

6. Kubinakova E, Danielik V, Hıves J. Electrochemical characterization of low-temperature molten mixture systems suitable as an innovation in aluminum technology. J Electrochem Soc. 2018;165(14):274. doi:10.1016/j.electacta.2018.01.174

7. Redkin A, Apisarov A, Dedyukhin A, Kovrov V, Zaikov Yu, Tkacheva O, Hryn J. Recent developments in low-temperature electrolysis of aluminum. ECS Trans. 2012;50(11):205–213. doi:10.1016/j.molliq.2017.02.021

8. Apisarov A, Dedyukhin A, Red'kin A, Tkacheva O, Zaikov Yu. Physicochemical properties of $KF-NaF-AlF_3$ molten electrolytes. Russ J Electrochem. 2010;46(6):633–639. doi:10.1134/S1023193510060066

9. Beck TR, MacRAE CM, Wilson NC. Metal anode performance in low-temperature electrolytes for aluminum production. Met Mater Trans B. 2011;42(4):807–813. doi:10.1007/s11663-011-9511-8

10. Tkacheva O, Hryn J, Spangenberger J, Davis B, Alcorn T. Operating Parameters of Aluminum Electrolysis in a $KF-AlF_3$ based Electrolyte. Light Met. 2012;675–680. doi:10.1007/978-3-319-48179-1_116

11. Hryn J, Tkacheva O, Spangenberger J. Initial 1000A aluminum electrolysis testing in potassium cryolite-based electrolyte. Light Met. 2016;1289–1294. doi:10.1007/978-3-319-65136-1_217

12. Zaikov Yu, Khramov A, Kovrov V, Kryukovsky V, Apisarov A, Chemesov O, Shurov N, Tkacheva O. Electrolysis of aluminum in the low melting electrolytes based on potassium cryolite. Light Met. 2009;505.

13. Cui P, Solheim A, Haarberg GM. The performance of aluminium electrolysis in a low temperature electrolyte system. Light Met. 2016;383–387. doi:10.1007/978-3-319-48251-4_63

14. Yasinskiy AS, Padamata SK, Polyakov PV, Shabanov AV. An update on inert anodes for aluminium electrolysis. Nonferrous Met.2020;48(1):15–23. doi:10.17580/nfm.2020.01.03

15. Helle S, Brodu B, Davis B, Guay D, Roue L. Influence of the iron content in Cu–Ni based inert anodes on their corrosion resistance for aluminium electrolysis. Corros Sci. 2011;53(11):3248–3253. doi:10.1016/j.corsci.2011.05.069

16. Nguyen T, de Nora V. De Nora oxygen evolving inert metallic anode. Light Met. 2006;385–390.

17. Glucina M, Hyland M, Laboratory-scale performance of a binary Cu–Al alloy as an anode for aluminium electrowinning. Corros Sci. 2006.48(9):2457–2469. doi:10.1016/j.corsci.2005.09.013

18. Bradford DR. Inert anode metal life in low temperature reduction process. Nat Tech Rep Lib. 2005;101. Available from: https://ntrl.ntis.gov/NTRL/dashboard/searchResults/titleDetail/DE2006841153.xhtml

19. Suzdaltsev AV, Nikolaev AYu, Zaikov YuP. Towards the stability of low-temperature aluminum electrolysis. J Electrochem Soc. 2021;168(4);046521. doi:10.1149/1945-7111/abf87f

20. Wang J, Lai Y, Tian Z, Liu Y. Effect of electrolysis superheat degree on anticorrosion performance of $5Cu/(10NiO-NiFe_2O_4)$ cermet inert anode. J Cent South Univ Technol. 2007;14(6):768–772. doi:10.1007/s11771-007-0146-5

21. Nikolaev AYu, Suzdaltsev AV, Polyakov PV, Zaikov YuP. Cathode process at the electrolysis of $KF-AlF_3-Al_2O_3$ melts and suspensions. J Electrochem Soc. 2017;164(8):S315–5321. doi:10.1149/2.0491708jes

22. Pawlek RP. Wettable cathodes: an update. Essen Read Light Met. 2010;4;1185–1190. doi:10.1007/978-3-319-48200-2_157

23. Brown CV. Final Report: Wetted Cathodes for Low-Temperature Aluminum Smelting. Mater Sci. 2002;51. doi:10.2172/801562

24. Rybakova N, Souto M, Martinz HP, Andriyko Y, Artner W, Godinho J, Nauer GE. Stability of electroplated titanium diboride coatings in high-temperature corrosive media. Corros Sci. 2009;51(6):1315–1321. doi:10.1016/j.corsci.2009.03.020

25. Rybakova N, Souto M, Martinz HP, Andriyko Y, Artner W, Godinho J, Nauer GE. Morphology and mechanical properties of tib2 coatings deposited from chloride-fluoride melts by pulse electroplating. J Electrochem Soc. 2009;156(4):131. doi:10.1149/1.3060508

26. Sista V, Kahvecioglu O, Kartal G, Zeng QZ, Kim JH, Eryilmaz OL, Erdemir A. Evaluation of electrochemical bonding of Inconel 600. Surf Coat Technol. 2013;215:452–549. doi:10.1016/j.surfcoat.2012.08.083

27. Kartal G, Eryilmaz OL, Krumdick G, Erdemir A, Timur S. Kinetics of electrochemical boriding of low carbon steel. Appl Surf Sci. 2011;257(15):6928–6934. doi:10.1016/j.apsusc.2011.03.034

28. Polyakova LP, Bukatova GA, Polyakova EG, Christensen E, Barner JH, Bjerrum N. Electrochemical behavior of boron in LiF-NaF-KF- melts. J Electrochem Soc. 1996;143(10):3178–3191. doi:10.1149/1.1837184

29. Raj SC, Skyllas-KIazacos M. Electrochemical studies of the effect of tio2 and b2o3 additions on the aluminum deposition reaction in the molten cryolite bath. Electrochim Acta. 1992;37(10):17871796. doi:10.1016/0013-4686(92)85082-V

30. Kataev AA, Karimov KR, Chernov YaB, Kulik NP, Malkov VB, Antonov BD, Vovkotrub EG, Zaikov YuP. Wetting of boride cathode coatings by low-melting-point cryolite and liquid aluminum. Rus Met. 2010;8:689–701. doi:10.1134/S0036029510080057

31. Kataev A, Tkacheva O, Molchanova N, ZaikovYu. Production of the Al–B Master alloy by aluminothermal reduction of KBF_4 and B_2O_3 in a medium of the molten salt flux. Russ J Non-Ferrous Met. 2019;60(4):354–362. doi:10.3103/S1067821219040059

32. Chrenkova M, Danek V, Vasiljev R, Silny A, Kremenetsky V,Polyakov E. Density and viscosity of the $(LiF-NaF-KF)(eut)-KBF_4-B_2O_3$ melts. J Mol Liq. 2003;102(1–3):213–226. doi:10.1016/S0167-7322(02)00063-6

33. Kataev AA, Rudenko AV, Reznitskikh OG, Molchanova NG, Dedyukhin AE, Redkin AA, Zaikov OYu. Thermal stability of KBF_4 in fusible cryolite melts. Rasplavy. 2014;6(12):12–17.

34. Nikolaev A, Suzdaltsev A, Zaikov Yu. Cathode process in the $KF-AlF_3-Al_2O_3$ melts. J Electrochem Soc. 2019;166(15):784–791. doi:10.1149/2.0521915jes

35. Keniry J. The economics of inert anodes and wettable cathodes for aluminum reduction cells. JOM. 2001;5:43–47. doi:10.1007/s11837-001-0209-2

36. Filatov AA, Suzdaltsev AV, Zaikov YuP. Cathode processes in the $KF-AlF_3-Al_2O_3-B_2O_3$ melt. Rasplavy. 2022;1:61–72. doi:10.31857/S0235010622010030

37. Kataev AA, Tkacheva OYu, Molchanova NG, Zaikov YuP. Production of the Al–B Master alloy by aluminothermal reduction of KBF_4 and B_2O_3 in a medium of the molten salt flux Russ J Non-Ferrous Met.2019;60(4),354–362. doi:10.3103/S1067821219040059

38. Wang X. Boride phase formation in the production of Al-B master alloys. J Alloys Compd. 2017;722:302–306. doi:10.1016/j.jallcom.2017.06.107